# Dynamics of optical nonlinearity of Ge nanocrystals in a silica matrix

Y. X. Jie, Y. N. Xiong, A. T. S. Wee,[a] C. H. A. Huan, and W. Ji
*Department of Physics, National University of Singapore, Kent Ridge, Singapore 119260*

(Received 4 May 2000; accepted for publication 13 October 2000)

The optical nonlinearity and excited carrier lifetime in Ge nanocrystals (*nc*-Ge) embedded in a silica matrix have been investigated by means of single beam *z* scan and pump-probe techniques with laser pulse duration of 35 ps and 532 nm wavelength. The *nc*-Ge samples were prepared using magnetron cosputtering and postgrowth annealing at 800 °C. The nonlinear absorption coefficient $\alpha_2$ and refractive index $n_2$ were found to range between 190 and 760 cm/GW, and 0.0026 and 0.0082 $cm^2$/GW, respectively, and be proportional to the Ge concentration in the film. The confined excited carriers were found to depopulate with a lifetime of ~70 ps. The nonlinearity in Ge nanocrystals is deduced to originate mainly from excited carrier absorption, with two-photon absorption providing a small contribution. © *2000 American Institute of Physics.* [S0003-6951(00)05249-9]

The linear and nonlinear optical properties of transparent thin films embedded with metal or semiconductor nanocrystals have been intensively studied since the mid-80s. It is well known that a transparent dielectric matrix containing metal nanocrystals, such as Au, Ag, and Cu, exhibit novel linear and nonlinear optical properties due to local field enhancement near the surface plasmon resonance of the metal.[1,2] In semiconductor nanocrystal embedded thin films, the energy structure of semiconductor nanocrystals, in particular the energy band gap can be varied in a broad range by altering the nanocrystal size. Meanwhile, three-dimensional quantum confinement results in discrete energy structures and atomic-like selection rules for interband and intraband optical transitions in semiconductor nanocrystals. Strong and fast optical nonlinearities, optical gain and lasing, tunable absorption, and strong photo- and electroluminescence, have been reported for these materials, making them attractive for potential applications in optoelectronics and signal processing.[3–9]

The nonlinear response from *nc*-Ge nanocrystals in a silica matrix formed by ion implantation and annealing has been previously reported using time-resolved degenerate-four-wave-mixing measurement.[3] Strong nonlinearity was observed and two characteristic relaxation times of nonlinear response were found, one at <100 fs and the other at ~1 ps. Neither of these two characteristic times can represent the excited carrier lifetime in the conduction band because the pump laser energy used (wavelength 800 nm) was not high enough to excite electrons from the bottom of the conduction band to the upper energy band. In this letter, we present an investigation of the nonlinear optical properties *nc*-Ge embedded in silica matrix formed by magnetron cosputtering and annealing using 532 nm picosecond laser pulses. This photon excitation energy is high enough to drive $\Gamma'_{25}\rightarrow\Gamma'_2$ and $\Gamma'_2\rightarrow\Gamma'_{15}$ transitions and is close to recent visible photoluminescence (PL) measurements.[4,8,9] Both the nonlinear absorption coefficient and refractive index were investigated with *Z*-scan measurements and the dynamics of optical nonlinearity was also investigated with pump-probe techniques.

The films were deposited by cosputtering in an argon ambient at room temperature using an Anelva (SPF-210H) sputtering system and postannealed at 800 °C. The annealing process consists of a 30 min temperature ramp, a 30 min anneal at the predetermined temperature, and a natural cooling process, as described in Ref. 7, to induce cubic *nc*-Ge formation. The Ge atomic concentration fractions in samples 1 to 4 were determined to be 8.5, 13.6, 14.7, and 27.6%, respectively, using a VG ESCALAB x-ray photoelectron spectroscopy instrument with a monochromatic Al$K\alpha$ x-ray source. The films were deposited on double-sided polished fused quartz substrates for transmission optical measurements and silicon (100) substrates for high-resolution transmission electron microscopy (HRTEM) imaging as in Ref. 10. Because the film thickness is around 1.4 $\mu$m, the influence of the substrate on film morphology should be insignificant.

The structural characterization was made using a Philips CM300 HRTEM operating at 300 kV. Cross-sectional samples were prepared by mechanical polishing, dimpling, and ion milling. Figure 1 shows the cross-sectional HRTEM image from the annealed sample 3. Those dark patches in Fig. 1 represent the Ge nanocrystals. Clear fringes corresponding to cubic nanocrystalline Ge [111] planes were also observed at a higher resolution.[7] The size distribution determined from this image is shown in the inset, which can be well represented by a lognormal function with a geometric mean diameter of 6.0 nm and a dimensionless geometric standard deviation of 1.8 nm. It can also be found from the TEM image that the *nc*-Ge are nearly uniformly distributed in the thin film.

Spectroscopic linear absorption spectra from these annealed samples with different Ge concentrations were also measured. The linear absorption by the silicon oxide film without Ge doping is negligible in both the visible and infrared range. However, when *nc*-Ge are present in the thin films, the spectra show two resonant absorption ramps at around ~1.2 and ~3.2 eV, respectively, which may correspond to the $\Gamma'_{25}\rightarrow\Gamma'_2$ ($\Delta E\sim 0.8$ eV) and $\Gamma'_{25}\rightarrow\Gamma'_{15}$ transitions ($\Delta E\sim 2.7-3.6$ eV) in bulk Ge.[3] Because there is a broad size distribution for the nanocrystals in our samples, we do not anticipate observing a sharp resonant absorption

[a]Electronic mail: phyweets@nus.edu.sg

 

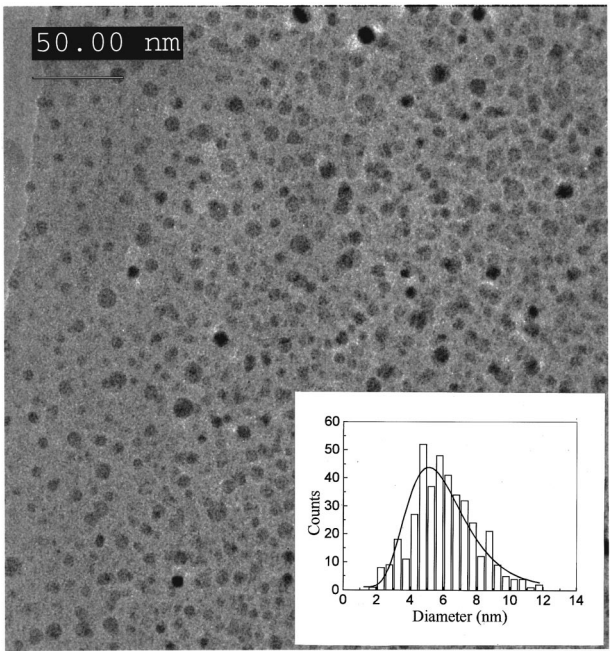


FIG. 1. HRTEM image of Ge nanocrystals with a diameter of $6 \pm 1.8$ nm in the sample with atomic Ge fraction of 14.7%. The inset figure represents the size distribution and a lognormal fit is shown as the solid line.

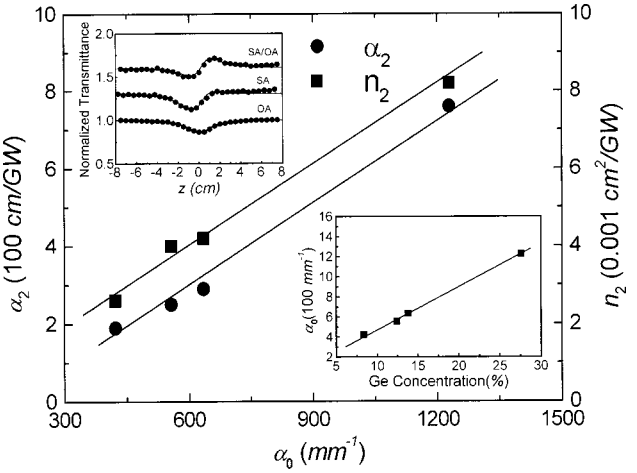


FIG. 2. The dependence between the intensity-dependent absorption coefficient ($\alpha_2$), refractive index ($n_2$) and the linear absorption coefficient ($\alpha_0$). The left inset shows $Z$ scans with (OA) and without an aperture (SA) and their division from the sample with 14.7% Ge with $I_p = 11.7$ GW/cm$^2$. The solid lines are the best fit. The right inset represents the relation between $\alpha_0$ and Ge concentration.

edge due to quantum confinement effects. However, a blueshift of the absorption edge was observed with a decrease in Ge concentration, and hence, *nc*-Ge size. This blueshift is consistent with the concept of quantum confinement.

We define the total absorption coefficient and the refractive index as $\alpha = \alpha_0 + \alpha_2 I$ and $n = n_0 + n_2 I$, respectively, where $\alpha$ and $n$ represent absorption and refractive coefficients, respectively, and subscripts 0 and 2 denote the linear and nonlinear ones. $I$ is the laser irradiance. We determine $\alpha_2$ and $n_2$ of the film by $z$-scan measurements.[11] The laser pulses at 532 nm wavelength with a repetition rate of 10 Hz were provided by a Q-switched, mode-locked, frequency-doubled Nd:yttrium–aluminum–garnet laser. The laser beam was focused by a ($f = 500$ mm) lens to a waist of 40 $\mu$m. The Rayleigh range $z_0$ of the beam was ~9 mm, much longer than the thickness of either the substrate or the film. Each $z$-scan spectrum was obtained by sampling 32 points along the $z$ axis in the range of 160 mm. At each $z$ position, the energy of the transmitted pulse (or the incident pulse) was sampled ten times, averaged and normalized to yield values for the normalized transmittance as a function of the $z$ position. Long-term thermal effects can be neglected because we conducted the experiments under the 10 Hz repetition rate and single-shot conditions and no obvious differences were observed. The nonlinear refraction and nonlinear absorption were separated by conducting $Z$ scan with and without an aperture in front of the detector. Nonlinearity could not be observed in the silicon oxide film without Ge doping at the peak irradiance $I_p$ up to 28 GW/cm$^2$. The left inset in Fig. 2 shows the $Z$ scans without [or, open aperture (OA)] and with the aperture [or, small aperture (SA)], and division of the SA $Z$ scan by the OA $Z$ scan for the annealed sample 3. The SA $Z$ scan indicates a positive value for $n_2$. The solid lines represent the best fit for the experimental data with $\alpha_2 = 290$ cm/GW and $n_2 = 0.0042$ cm$^2$/GW at $I_p = 11.7$ GW/cm$^2$. The two nonlinear parameters were observed to increase dramatically after the thermal annealing treatment. In particular, the nonlinear refractive index of the annealed sample becomes an order larger than that of the as-deposited sample. This result implies that the nonlinearity of these films is mainly from *nc*-Ge formed only after thermal annealing. The relations between $\alpha_2$ (or $n_2$) and $\alpha_0$ from the annealed samples are shown in Fig. 2. The right inset in Fig. 2 represents the relation between Ge concentration and $\alpha_0$. It can be seen that $\alpha_0$ is proportional to the Ge concentration and $\alpha_2$ and $n_2$ follow a linear relation with $\alpha_0$. This result is in agreement with the results reported in Ref. 3. It is also found that both $\alpha_2$ and $n_2$ are nearly independent of the pump laser intensity for $I_p$ up to ~20 GW/cm$^2$.

The dynamic response of the observed nonlinearity of the samples was examined by a standard pump and probe technique.[12] The incident 35 ps laser pulses were split into a pump pulse and a probe pulse by a beam splitter. The probe intensity was around 5% of the pump. The normalized transmittance of the probe beam from the annealed sample 3 was recorded as a function of the time delay $t$ between the pump and probe pulses as shown in Fig. 3. The scattered points represent the experimental data and the dotted curve represents the temporal profile of the pump pulse. Obviously, the probe transmittance does not recover immediately after the pump beam has passed through the sample. Furthermore, since the pump photon energy is higher than the energy band gap even after considering gap widening due to confinement effects for nanocrystals with size of 6 nm, this result suggested that excited carriers generated through linear absorption make a contribution to nonlinearity. Two-photon absorption from the $\Gamma'_{25} \rightarrow \Gamma'_{15}$ transitions may also contribute to the nonlinearity.[3] Therefore, the following equations may apply:

$$\frac{dN_e}{dt} = \frac{\beta_{2\mathrm{PA}} I^2}{2h\nu} + \frac{\alpha_0 I}{h\nu} - \frac{N_e}{\tau}, \tag{1}$$

$$\frac{dI}{dz} = -\beta_{2\mathrm{PA}} I^2 - \alpha_0 I - \sigma_a N_e I. \tag{2}$$

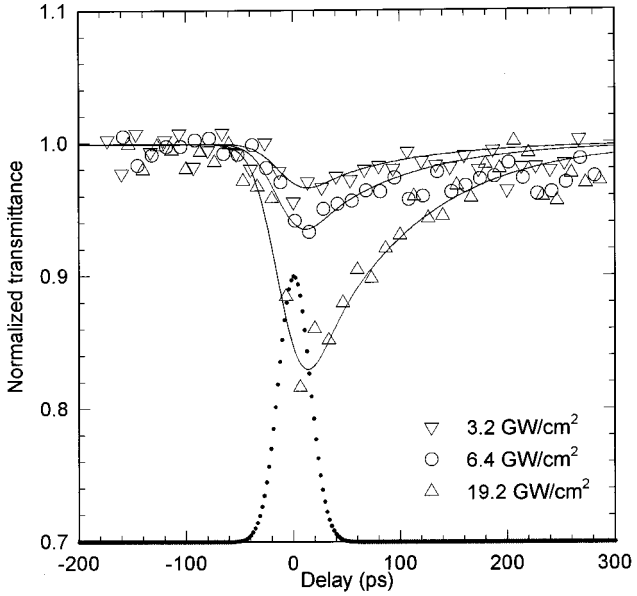


FIG. 3. The dynamic nonlinear responses from the sample with 14.7% Ge concentration with different $I_p$ up to 19.2 GW/cm$^2$.

Here, $\beta_{2PA}$ is the two-photon absorption coefficient and $I$ is the beam intensity. The excited carrier absorption cross section is represented with $\sigma_a$. $N_e$ is the excited carrier density, $\tau$ is the lifetime, and $I$ and $N_e$ are functions of $r$, $t$, and $z$. By assuming a $TEM_{00}$ Gaussian beam, the experimental data were numerically fitted with the earlier equations. The solid lines represent the calculated results with $\beta_{2PA} = 30$ cm/GW. The excited carrier lifetime confined in nanocrystals is about 70 ps for all pump laser intensities from 3.2 to 19.2 GW/cm$^2$. From the *Z*-scan results on the same sample, the two-photon absorption contribution is only ~10% of that from excited carriers. Therefore, the nonlinearity of the sample is mainly from linear absorption generated excited carrier with a small contribution from two-photon absorption. However, the contribution to the nonlinear optical properties from excited carriers generated through two-photon absorption can be disregarded for the laser intensities up to 19.2 GW/cm$^2$, which is in agreement with our previous intensity independent *Z*-scan result.

The excited carrier lifetime in *nc*-Ge is close to the reported excited carrier lifetime of CdSe and CdS nanocrystals. Klimov *et al.* used a similar method to study the excited carrier lifetime of CdSe and CdS nanocrystals and found the lifetime to be ~40 ps which is strongly dependent on the nanocrystal surface passivation.[13,14] They also deduced that the excited carrier relaxation is mainly due to electron trapping at the surface localized defects.[13] PL decay times are ~1 ns for both the blue, orange-green and near infrared bands.[4–6] This time interval is much longer than the excited carrier lifetime we determined from our time resolved pump-probe experiment. In other words, the excited carriers generated by linear absorption in the nanocrystals depopulate much faster than radiative recombination. The discrepancy between the excited carrier lifetime and the reported PL decay time suggests that the excited carrier generation and radiative recombination do not take place simultaneously or at the same place. Therefore, we postulate that the excited carriers in Ge nanocrystals mainly depopulate through surface trapping at surface localized defects as in CdSe and CdS nanocrystals. This conclusion is also consistent with defect-related PL mechanism for large Ge nanocrystal sizes (>~5 nm).[8,9]

The detected relaxation of nonlinear response in our samples is on a slower time scale than that reported in Ref. 3. However, the nonlinearity in our samples indicates a similar Ge concentration dependence as in Ref. 3. Moreover, the nonlinear refractive response time in Ref. 3 is longer than the laser pulse width. Therefore, it appears that the mechanism of nonlinear response in Ref. 3 may also originate from excited carrier and two-photon absorption. The lifetime difference suggests that the 1 ps time scale characterizes a different ultrafast process. Since the energy required for the $\Gamma_2' \rightarrow \Gamma_{15}'$ transition is >2 eV[15,16] and even larger after considering quantum confinement effects, which is larger than their pump laser photon energy (wavelength 800 nm), excited carriers near the bottom of conduction band could not contribute to the nonlinearity. Therefore, the 1 ps time scale may represent the relaxation of excited carriers to bottom of the conduction band through phonon scattering. This is in agreement with the time scale for relaxation of nonequilibrium semiconductor plasma to quasi-equilibrium condition by electron-phonon scattering.[17] This would also be in consistent with the reported intraband transition lifetime in Ref. 10.

In summary, we have studied the nonlinearity of *nc*-Ge embedded in silicon oxide thin films using *Z* scan and pump-probe technique with 532 nm ps laser pulses. The nonlinear refractive index and absorption coefficient are Ge concentration dependent and range between 0.0026 and 0.0082 cm$^2$/GW and 190 and 760 cm/GW, respectively when the Ge atomic fraction increases from 8.5% to 27.6%. The nonlinearity mainly comes from excited carriers and two-photon absorption makes a small contribution. The excited carrier lifetime was determined to be ~70 ps and independent of laser intensity up to 19.2 GW/cm$^2$.

[1] J. M. Ballesteros, R. Serna, J. Solís, C. N. Afonso, A. K. Petford-Long, D. H. Osborne, and R. F. Haglund, Jr., Appl. Phys. Lett. **71**, 2445 (1997).
[2] S. Banerjee and D. Chakravorty, Appl. Phys. Lett. **72**, 1027 (1998).
[3] A. Dowd, R. G. Elliman, M. Samoc, and B. Luther-Davies, Appl. Phys. Lett. **74**, 239 (1999).
[4] Y. Kanemitsu, H. Uto, Y. Masumoto, and Y. Maeda, Appl. Phys. Lett. **61**, 2187 (1992).
[5] M. Zacharias and P. M. Fauchet, Appl. Phys. Lett. **71**, 380 (1997).
[6] S. Takeoka, M. Fujii, S. Hayashi, and K. Yamamoto, Appl. Phys. Lett. **74**, 1558 (1999).
[7] Y. X. Jie, A. T. S. Wee, C. H. A. Huan, S. P. Ng, and W. K. Choi (unpublished).
[8] S. Y. Ma, Z. C. Ma, W. H. Zong, G. Qin, and G. G. Qin, J. Appl. Phys. **84**, 559 (1998).
[9] K. S. Min, K. V. Shcheglov, C. M. Yang, H. A. Atwater, M. L. Brongersma, and A. Polman, Appl. Phys. Lett. **68**, 2511 (1996).
[10] S. Takeoka, K. Toshikiyo, M. Fujii, S. Hayashi, and K. Yamamoto, Phys. Rev. B **61**, 15988 (2000).
[11] M. Sheik-Bahae, A. A. Said, T. Wei, D. J. Hagan, and E. W. Van Stryland, IEEE J. Quantum Electron. **26**, 760 (1990).
[12] T. Xia, A. Dogariu, K. Mansour, D. J. Hagan, A. A. Said, E. W. Van Stryland, and S. Shi, J. Opt. Soc. Am. B **15**, 1497 (1998).
[13] V. I. Klimov, Ch. J. Schwarz, D. W. McBranch, C. A. Leatherdale, and M. G. Bawendi, Phys. Rev. B **60**, R2177 (1999).
[14] V. Klimov and D. McBranch, Phys. Rev. Lett. **80**, 4028 (1998).
[15] M. L. Cohen and J. R. Chelikowsky, *Electronic Structure and Optical Properties of Semiconductors*, 2nd ed. (Springer, Berlin, 1989).
[16] P. Tognini, A. Stella, S. De Silvestri, M. Nisoli, S. Stagira, P. Cheyssac, and R. Kofman, Appl. Phys. Lett. **75**, 208 (1999).
[17] J. Wang, M. Sheik-Bahae, A. A. Said, D. J. Hagan, and E. W. Van Stryland, J. Opt. Soc. Am. B **11**, 1009 (1994).